

Dielectric behavior of $\text{Bi}_{2/3}\text{Cu}_3\text{Ti}_4\text{O}_{12}$ ceramic and thick films

D. Szwagierczak

Received: 31 May 2007 / Accepted: 20 June 2008 / Published online: 11 July 2008
© Springer Science + Business Media, LLC 2008

Abstract The paper reports on synthesis, sintering and microstructure of $\text{Bi}_{2/3}\text{Cu}_3\text{Ti}_4\text{O}_{12}$, a lead-free, high-permittivity material with internal barrier layer capacitor behavior. Complex impedance and capacitance of the ceramic and thick films were studied as a function of frequency (10 Hz–2 MHz) and temperature (–170 to 400°C). Dc electrical conductivity of the samples was measured in the temperature range 20–400°C. Broad and high maxima of dielectric permittivity versus temperature plots were observed reaching 60,000 for ceramic and 5,000 for thick films. The maxima decrease and shift to higher temperatures with increasing frequency. Two arcs ascribed to grains and grain boundaries were found in the plots of imaginary part versus real part of impedance. Analysis of the impedance spectra indicates that $\text{Bi}_{2/3}\text{Cu}_3\text{Ti}_4\text{O}_{12}$ ceramic could be regarded as electrically heterogeneous system composed of semiconducting grains and less conducting grain boundaries. The developed thick film capacitors with dielectric layers based on $\text{Bi}_{2/3}\text{Cu}_3\text{Ti}_4\text{O}_{12}$ exhibit dense microstructure, good cooperation with Ag electrodes, high permittivity up to 5,000 and relatively low temperature coefficient of capacitance in the temperature range 100–300°C. Broad maxima in the dielectric permittivity versus temperature curves may be attributed to Maxwell–Wagner relaxation.

Keywords $\text{Bi}_{2/3}\text{Cu}_3\text{Ti}_4\text{O}_{12}$ ceramic · Thick films · Dielectric response · Internal barrier layer capacitor

1 Introduction

Strong demand for miniaturization of capacitive elements and elimination of lead based compounds have caused great attention being gained by the so-called high-k materials. For many years ferroelectrics or relaxors containing lead have been commercially used as high ϵ capacitor materials. Recently, several new nonferroelectric lead-free compounds, such as $\text{CaCu}_3\text{Ti}_4\text{O}_{12}$ [1–6], $\text{Cu}_2\text{Ta}_4\text{O}_{12}$ [7], $\text{AFe}_{1/2}\text{B}_{1/2}\text{O}_3$ ($A=\text{Ba}$, Sr , Ca ; $B=\text{Nb}$, Ta , Sb) [8], $\text{Bi}_{2/3}\text{Cu}_3\text{Ti}_4\text{O}_{12}$ [9, 10], have been intensively studied due to their high dielectric permittivity, almost independent of temperature and frequency over a broad range. Origin of this behavior has been attributed to Maxwell–Wagner polarization mechanism. $\text{CaCu}_3\text{Ti}_4\text{O}_{12}$ (CCTO) in the form of single crystal, ceramic and thin films has been subject of many theoretical and experimental works [1–6]. Cohen et al. [1] suggested that large, temperature independent low-frequency dielectric constant observed in single crystal CCTO stems from spacial inhomogeneities of local dielectric response. Probable sources of these inhomogeneities may be twins, compositional ordering or antiphase boundaries. Six possible morphologies have been distinguished which could lead to the observed dielectric behavior. The domains can be conducting or insulating in bulk. If the domains are conducting, their boundaries must be insulating (blocking) and vice versa. The conductive bulk can be percolating or below the percolation threshold. The barrier layers at boundaries can be intrinsic or associated with electrode-sample interface. Sinclair et al. [2] basing on impedance spectroscopy studies stated that CCTO ceramic is a one step internal barrier layer capacitor (IBLC) with conductive grains and insulating grain boundaries. Zhang and Tang [3] showed that variable range hopping (VRH) mechanism is responsible

D. Szwagierczak (✉)
Cracow Division, Institute of Electron Technology,
Zabłocie 39,
30-701 Kraków, Poland
e-mail: dszwagi@ite.waw.pl

for bulk dc conductivity in CCTO ceramics. Frequency response of CCTO thin films grown epitaxially on LaAlO₃ substrate by Tselev et al. [4] was found to be dominated by power-law, typical of localized hopping charge carriers.

Giant and nearly temperature independent dielectric constant values reaching 10^4 – 10^5 at low frequencies and/or at high temperatures were found also for single crystals of copper tantalum oxide Cu₂Ta₄O₁₂ by Renner et al. [7] and ascribed to surface barrier layer capacitors (SBLC) formation at the sample-electrode interface.

Raevski et al. [8] proposed that very high values of dielectric permittivity of AFe_{1/2}B_{1/2}O₃ ceramics (A =Ba, Sr, Ca; B =Nb, Ta, Sb) observed in a wide temperature interval are due to the Maxwell–Wagner relaxation.

The literature data concerning Bi_{2/3}Cu₃Ti₄O₁₂ are scarcely available [9, 10]. Subramanian et al. [9] found that more than ten compounds in the ACu₃M₄O₁₂ system, among them Bi_{2/3}Cu₃Ti₄O₁₂, exhibit large dielectric constant values exceeding 1,000 at room temperature.

In the cubic perovskite-like structure of Bi_{2/3}Cu₃Ti₄O₁₂ 1/3 of Bi sites are vacant to ensure charge neutrality [10].

Liu et al. [10] studied impedance, electric modulus and dielectric permittivity of Bi_{2/3}Cu₃Ti₄O₁₂ ceramic in the temperature range from –150°C to 200°C and frequency range from 10^{–1} to 10⁶ Hz. Two responses were found in impedance and modulus formalisms, attributed to the grains and to grain boundaries. First set of weak peaks in the frequency dependence of the imaginary part Z'' of impedance was observed between –150°C and –70°C and the second set of maxima was revealed above 0°C. Segments of a small arc and a big arc could be distinguished in log $Z''=f(\log Z')$ plots below –100°C. The ratio of diameters of two arcs higher than 10⁵ indicates that the grain resistance R_g , related to the smaller arc, is much lower than that associated with grain boundaries R_{gb} , represented by the big arc. On the basis of frequency dependencies of M'' Liu et al. [10] concluded that grain capacitance is approximately ten times smaller than that of grain boundaries. Dielectric permittivity ϵ' decreases from a constant higher level at low frequencies to a small value at high frequencies. ϵ'' exhibits a Debye-like relaxation maxima shifting towards higher frequencies as temperature increases. Liu et al. [10] ascribed these maxima to Maxwell–Wagner relaxation arising from electrical heterogeneity of the system consisting of conducting grains and poorly conducting grain boundaries.

The subject of this paper was the development of optimal conditions for synthesis and sintering of Bi_{2/3}Cu₃Ti₄O₁₂ ceramic, as well as the study of dielectric response of this material in dielectric permittivity, electric modulus, impedance and admittance formalisms. The work was also aimed at fabrication and characterization of dielectric layers destined for thick film capacitors.

2 Experimental

Starting materials Bi₂O₃, CuO and TiO₂ were mixed in appropriate proportions, ball-milled in isopropyl alcohol, dried, pelletized and calcined at 900°C for 5 h. The synthesized product was milled, mixed with 3% water solution of polyvinyl alcohol, granulated, pressed into discs and sintered at 980–1000°C during 2 h. Phase composition of the ceramic was analyzed by a Philips X'Pert diffractometer. Ceramic Bi_{2/3}Cu₃Ti₄O₁₂ samples were covered with screen printed silver electrodes, fired at 850°C.

The Bi_{2/3}Cu₃Ti₄O₁₂ powder after milling was also used for manufacturing pastes destined for dielectric layers in thick film capacitors. The pastes were prepared by mixing the ceramic powder with 40 wt.% of the solution of ethyl cellulose in terpineol and subsequent grinding in an agate mortar. Thick film capacitors were screen printed on alumina substrates. Bottom and top electrodes were deposited using Ag paste. The dielectric layers were printed through a 260-mesh screen, dried and fired in a VI-zone BTU belt furnace for 10 min at peak temperature of 850°C. The printing-drying-firing cycle was carried out three times. The thickness of the dielectric layers examined by means of a profilograph was about 20 μ m.

Complex impedance Z^* , permittivity ϵ^* and electric modulus M^* ($M^*=1/\epsilon^*$) of Bi_{2/3}Cu₃Ti₄O₁₂ ceramic and thick film samples were determined in the temperature range from –170 to 400°C as a function of frequency in the range 10 Hz–2 MHz, using a LCR QuadTech meter. Dc conductivity of the examined material was also measured in the temperature range 20–400°C by means of a Philips resistance meter.

A FEI scanning electron microscope was applied to examine the microstructure of Bi_{2/3}Cu₃Ti₄O₁₂ ceramic and thick films.

3 Results and discussion

X-ray diffraction analysis has confirmed single phase composition of the obtained Bi_{2/3}Cu₃Ti₄O₁₂ ceramic. Fig. 1 illustrates the fine-grained, dense microstructure of a ceramic sample sintered at 1000°C. As can be seen from Fig. 1(a), the grain sizes are not uniform, ranging from 0.5 to 4 μ m.

Impedance spectroscopy, as a method for measuring the response of a sample to a small applied sinusoidal voltage, provides a useful tool to distinguish electrically different regions in the examined sample over a wide range of frequencies. Ceramic materials can be usually well represented by the equivalent circuit consisting of a series connection of two parallel RC elements corresponding to grain bulk and grain boundaries.

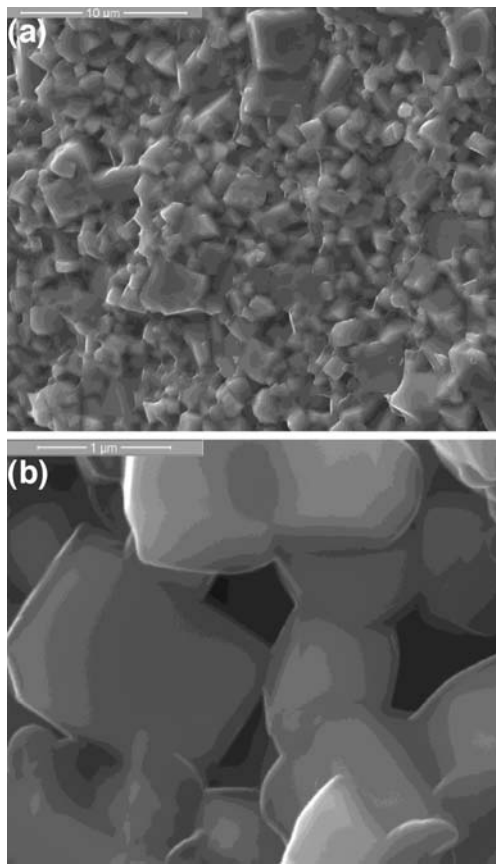


Fig. 1 SEM microphotograph of a fractured cross-section of $\text{Bi}_{2/3}\text{Cu}_3\text{Ti}_4\text{O}_{12}$ ceramic

Frequency dependencies of the real and the imaginary parts of impedance for $\text{Bi}_{2/3}\text{Cu}_3\text{Ti}_4\text{O}_{12}$ ceramic are shown in Figs. 2(a,b). In the $\log Z'$ versus $\log f$ plots a region of the almost constant level of the real part of impedance at low frequencies is followed by a region of a distinct drop and dispersion of Z' values. Frequency dependencies of the imaginary part of impedance exhibit two broad peaks decreasing and shifting to higher frequencies as temperature rises. Maxima in $\log Z''$ versus $\log f$ curves are broadened on the low frequency side of the peaks, indicating departure from the ideal Debye-like response. High frequency flat maxima, ascribed to the dielectric response of the grains, can be seen at temperatures below -90°C . At higher temperatures, above 50°C , there occur more distinct peaks attributed to grain boundaries.

Figure 3(a,b) present, for a few fixed temperatures from a low and a high temperature range, the relationship between the imaginary and the real parts of impedance in the linear coordinates. In the temperature range from -170 to 100°C a small arc attributed to grains and a part of the big arc due to grain boundaries are observed [Fig. 3(a)]. As illustrated in Fig. 3(b) for 150, 200 and 250°C , at higher temperatures only one arc related to grain boundaries is visible. The nonzero intercept of this arc with Z' axis,

shown in the inset in Fig. 3(b), suggests the existence of a second arc with f_{max} lying outside the available frequency range. The arcs in $Z''=f(Z')$ plots become smaller and shift to higher frequencies with increasing temperature, due to decreasing resistances. As displayed in Fig. 4, the resistances of grain boundaries R_{gb} and grains R_{g} , determined on the basis of the intercepts of the arcs with Z' axis, in the examined temperature range follow well Arrhenius law. The relevant activation energies are 0.55 and 0.073 eV for grain boundaries and grains, respectively. The latter value is typical of polaron relaxation in perovskites [11]. The activation energy for resistance of grain boundaries calculated on the basis of the impedance plots (0.55 eV) is consistent with the E value determined from dc conductivity measurements (0.55 eV), as can be seen comparing Figs. 4 and 5. The resistances of grains are 1–5 orders lower than those of grain boundaries. The mechanism of the formation of conducting grains is suggested to be related to small oxygen loss during sintering process and

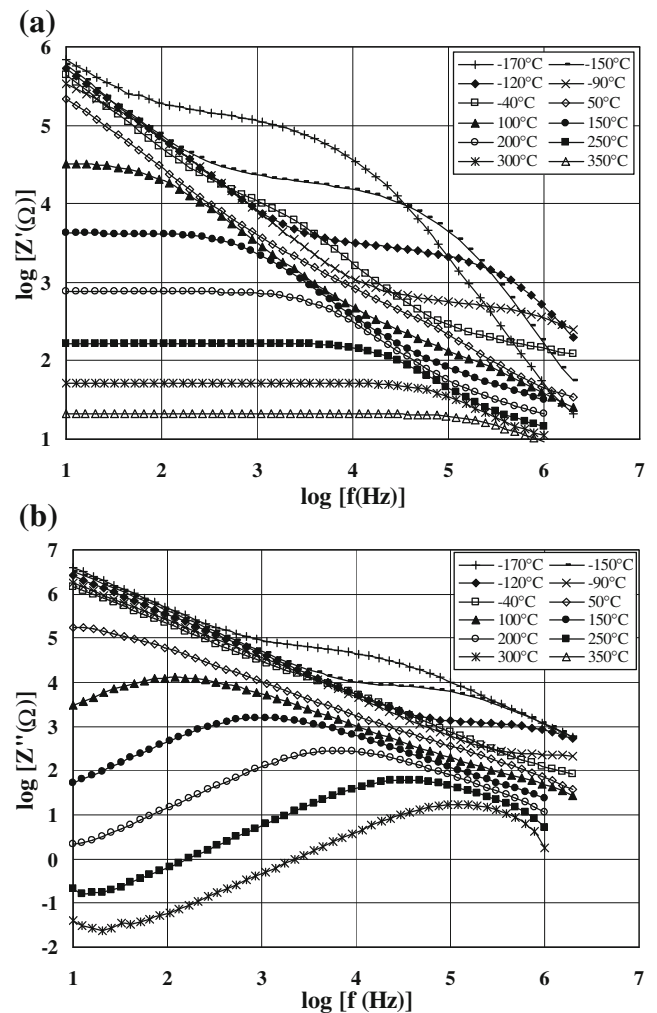


Fig. 2 Frequency dependence of the real part (a) and imaginary part (b) of impedance for $\text{Bi}_{2/3}\text{Cu}_3\text{Ti}_4\text{O}_{12}$ ceramic in the temperature range from -170 to 350°C

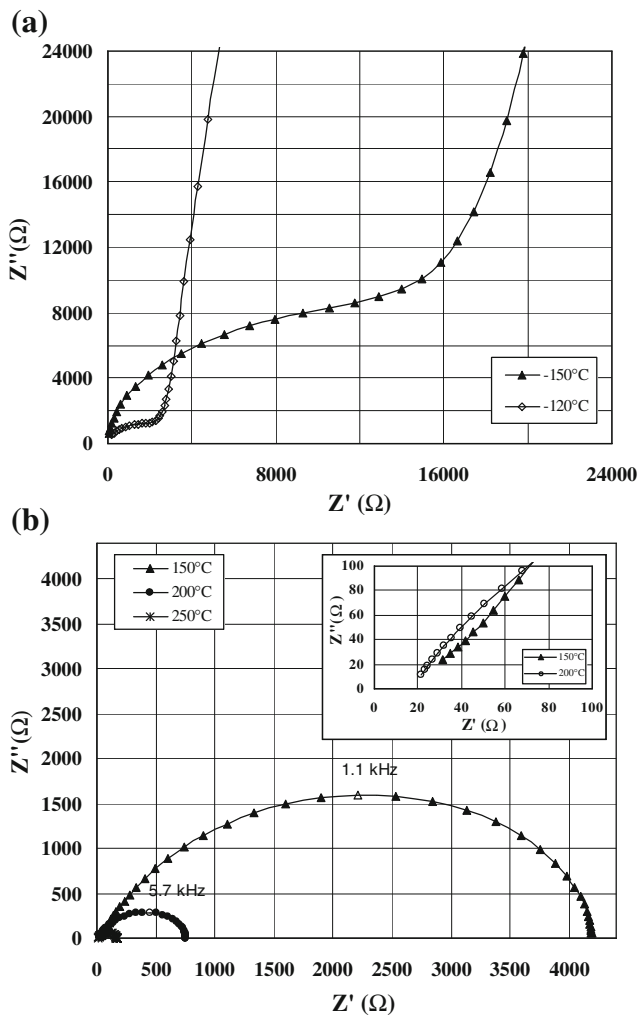


Fig. 3 Z'' versus Z' plots for $\text{Bi}_{2/3}\text{Cu}_3\text{Ti}_4\text{O}_{12}$ ceramic (a) at -150 and -120°C (b) at 150 , 200 and 250°C

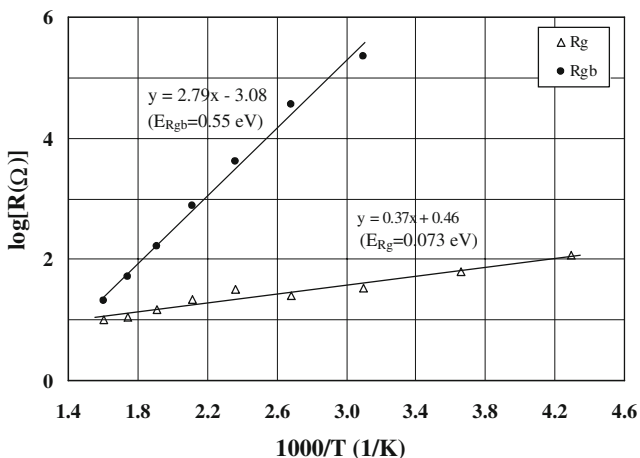


Fig. 4 Resistances of grains and grain boundaries for $\text{Bi}_{2/3}\text{Cu}_3\text{Ti}_4\text{O}_{12}$ ceramic as a function of reciprocal temperature

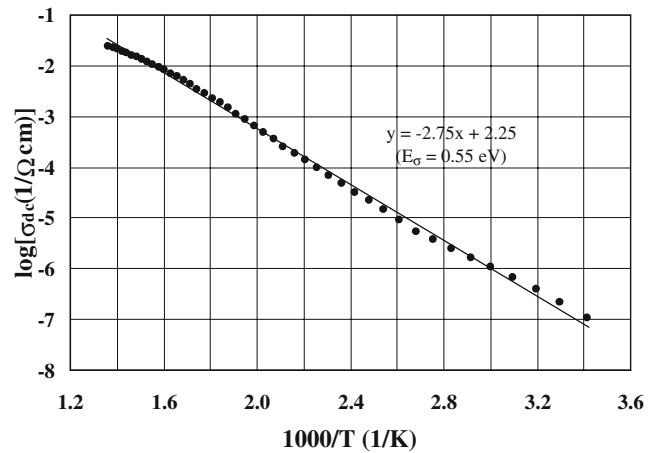


Fig. 5 Dc conductivity of $\text{Bi}_{2/3}\text{Cu}_3\text{Ti}_4\text{O}_{12}$ ceramic as a function of reciprocal temperature

partial reduction of Cu^{2+} to Cu^+ at high temperature. Reoxidation during cooling which occurs mainly at grain boundaries regions leads to higher resistivity of grain boundaries.

In Fig. 6 relaxation times for grain boundaries τ_{gb} estimated on the basis of the relationship $2\pi f_{\text{max}}\tau=1$ from the $Z''=f(Z')$ arcs are depicted versus reciprocal temperature. The activation energy derived from the Arrhenius plot is 0.60 eV. This value is lower than that reported by Liu et al. [10] for $\text{Bi}_{2/3}\text{Cu}_3\text{Ti}_4\text{O}_{12}$ ceramic (0.73 eV) and close to the activation energy determined by Sinclair et al. [2] for $\text{CaCu}_3\text{Ti}_4\text{O}_{12}$ ceramic (0.60 eV).

In Fig. 7 temperature dependence of dielectric permittivity ϵ' is presented for six fixed frequencies from the range 10 Hz– 1 MHz. In $\epsilon'=f(T)$ curves broad maxima are observed, decreasing and shifting to higher temperatures for measuring frequencies up to 100 kHz. Maxima in $\epsilon'=f(T)$ plots can be attributed to Debye-like relaxation of Maxwell–Wagner polarization. Broadening of these peaks is

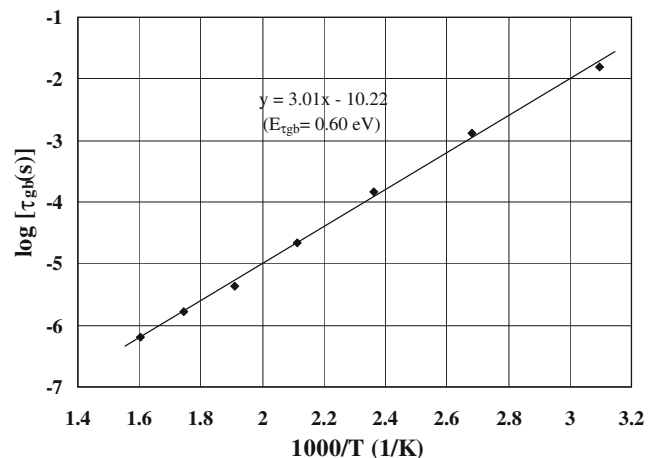


Fig. 6 Relaxation times for grain boundaries determined from the maxima of $Z''=f(Z')$ plots versus reciprocal temperature

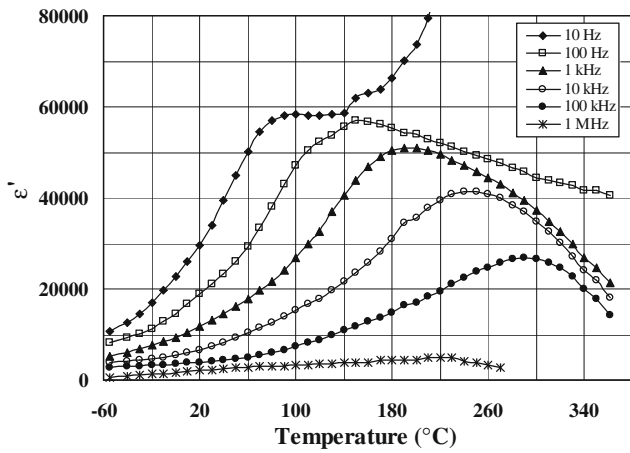


Fig. 7 Real part of permittivity of $\text{Bi}_{2/3}\text{Cu}_3\text{Ti}_4\text{O}_{12}$ ceramic versus temperature

presumably related to distribution of relaxation times resulting from distribution of grain sizes observed in SEM images. The maximum ϵ' values change from 5,000 at 1 MHz to 60,000 at 10 Hz.

At high frequencies and low temperatures the frequency dependences of permittivity drop and converge to a relatively high level of ϵ' exceeding 200, corresponding to the intrinsic properties of grains.

At lower temperatures the logarithm of ac conductivity increases almost linearly with increasing frequency, while at higher temperatures it becomes almost frequency independent. A region of frequency independence at low frequencies is followed by a region of a linear increase in logarithm of the real part of conductivity, according to the universal power law ($\sigma_{AC} \propto f^n$, $1 < n < 0$). The location of low-frequency plateau is strongly temperature dependent, shifting to higher frequencies with increasing temperature, whereas the n value, derived from the slope of the linear

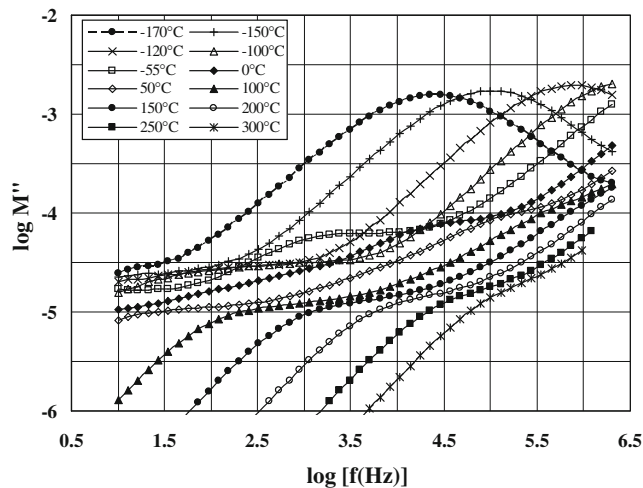


Fig. 8 Imaginary part of electric modulus versus frequency for $\text{Bi}_{2/3}\text{Cu}_3\text{Ti}_4\text{O}_{12}$ ceramic in the temperature range from -170 to 300°C

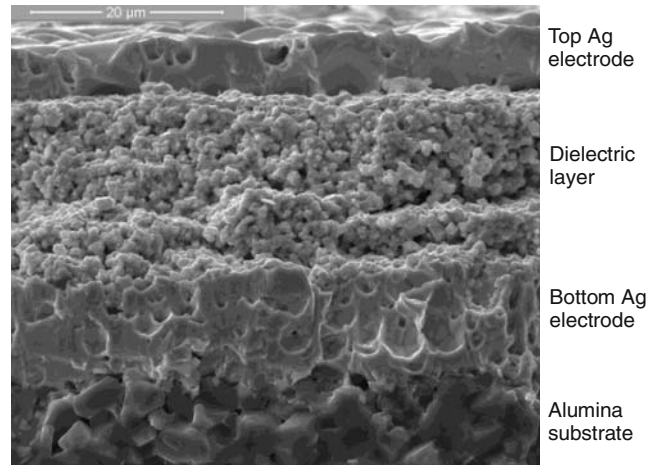


Fig. 9 SEM microphotograph of the fractured cross-section of a thick film capacitor with $\text{Bi}_{2/3}\text{Cu}_3\text{Ti}_4\text{O}_{12}$ dielectric layer

part of the plot, is almost temperature independent. The n value was found to be 0.7–0.77 in the temperature range 0 – 300°C .

As can be seen from Fig. 8, there are three sets of peaks in the plots of the imaginary part of electric modulus M'' versus frequency, shifting to higher temperatures with increasing frequency. Three dielectric responses can be distinguished—a distinct low temperature peak (below -100°C) attributed to grains, a flat medium temperature maximum (above -55°C), ascribed to grain boundaries and high temperature (low frequency) hump due probably to electrode-sample contact effects. Since the heights of the maxima are proportional to reciprocal capacitances, the capacitances related to grain boundaries were found to be ten times higher than those related to grains. The intensities of the maxima in all groups, and consequently capacitances of grains and grain boundaries, are almost temperature independent.

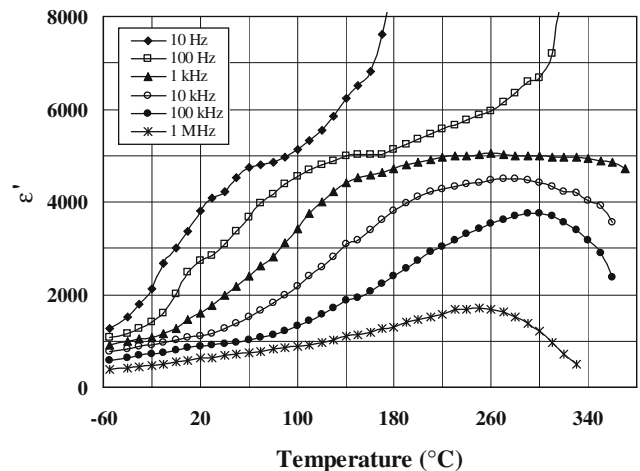


Fig. 10 Temperature dependence of the real part of permittivity for $\text{Bi}_{2/3}\text{Cu}_3\text{Ti}_4\text{O}_{12}$ thick films at frequencies 10 Hz–1 MHz

Figure 9 presents the fractured cross-section of a thick film capacitor based on $\text{Bi}_{2/3}\text{Cu}_3\text{Ti}_4\text{O}_{12}$ ceramic. The dielectric layer exhibits dense, fine-grained microstructure with no cracks or delamination at the boundaries with Ag electrodes. The majority of grains are finer than 1 μm . The average grain size is smaller than that for ceramic samples due to lower temperature and shorter time of sintering of layers as compared with the bulk ceramic.

Courses of the impedance spectra for thick films are quite similar to those for the bulk ceramic. Resistivities of grains and grain boundaries in the layers estimated from the maxima in $Z''=f(Z')$ plots are close to those for ceramic samples, decreasing from 800 to 200 Ωcm and from 10^7 to 800 Ωcm in the temperature range from -55 to 340°C .

In Fig. 10 temperature dependencies of the real part of permittivity are depicted for six fixed frequencies from the range 10 Hz–1 MHz for $\text{Bi}_{2/3}\text{Cu}_3\text{Ti}_4\text{O}_{12}$ thick films. Broad ε' maxima or humps are observed decreasing and shifting to higher temperatures for measuring frequencies up to 100 kHz. The maximum permittivity values in the frequency range 10 Hz–1 MHz are 1,700–5,000. The maxima are more flat and their heights are one order of magnitude lower than those for the ceramic samples. The permittivity drops rapidly with increasing frequency at low frequencies and then decreases slowly with a further frequency increase. The examined thick films exhibit advantageous, relatively low values of temperature coefficient of capacitance at the elevated temperature range 100–300°C (TCC $\leq \pm 20\%$).

Analyzing the impedance and permittivity data it can be stated that high dielectric permittivities of $\text{Bi}_{2/3}\text{Cu}_3\text{Ti}_4\text{O}_{12}$ ceramic and thick films stem from the creation of internal barrier layer capacitors consisting of semiconducting grains and less conductive grain boundaries.

4 Conclusions

$\text{Bi}_{2/3}\text{Cu}_3\text{Ti}_4\text{O}_{12}$ ceramic presented in this work is a promising lead-free, high capacitance material. Ceramic samples exhibit broad and high maxima in dielectric permittivity versus temperature plots, reaching 60,000 at low frequency. Two arcs were found in the complex plane impedance plots—attributed to grains, at temperatures

below 100°C , and those ascribed to grain boundaries at higher temperatures.

The developed thick film capacitors with dielectric layers based on $\text{Bi}_{2/3}\text{Cu}_3\text{Ti}_4\text{O}_{12}$ show dense microstructure, good cooperation with Ag electrodes, high permittivity up to 5,000 and relatively low temperature coefficient of capacitance in the temperature range 100–300°C. Broad maxima in the dielectric permittivity versus temperature curves may be ascribed to Maxwell Wagner relaxation.

The observed dielectric behavior of $\text{Bi}_{2/3}\text{Cu}_3\text{Ti}_4\text{O}_{12}$ ceramic and thick films is believed to be related to spontaneous formation, by a one-step procedure, of internal barrier layer capacitors, composed of semiconducting grains and less conducting grain boundaries.

Acknowledgements This work has been supported by Polish Ministry of Science and Higher Education under grant No. N507037 31/0906.

References

1. M.H. Cohen, J.B. Neaton, L. He, D. Vanderbilt, *J. Appl. Phys* **94**, 3299 (2003), doi:10.1063/1.1595708
2. D.C. Sinclair, T.B. Adams, F.D. Morrison, A.R. West, *Appl. Phys. Lett* **80**, 2153 (2002), doi:10.1063/1.1463211
3. L. Zhang, Z.-J. Tang, *Phys. Rev. B* **70**, 174306 (2004), doi:10.1103/PhysRevB.70.174306
4. A. Tselev, C.M. Brooks, S.M. Anlage, H. Zheng, L. Salamanca-Riba, R. Ramesh et al., *Phys. Rev. B* **70**, 144101 (2004), doi:10.1103/PhysRevB.70.144101
5. J. Li, A.W. Sleight, M.A. Subramanian, *Sol. Stat. Com* **135**, 260 (2005), doi:10.1016/j.ssc.2005.04.028
6. A.R. West, T.B. Adams, F.D. Morrison, D.C. Sinclair, *J. Eur. Ceram. Soc* **24**, 1439 (2004), doi:10.1016/S0955-2219(03)00510-7
7. B. Renner, P. Lunkenheimer, M. Schetter, A. Loidl, A. Reller, S. G. Ebbinghaus, *J. Appl. Phys* **96**, 4400 (2004), doi:10.1063/1.1787914
8. I.P. Raevski, S.A. Prosandeev, A.S. Bogatin, M.A. Malitskaya, L. Jastrabik, *J. Appl. Phys* **93**, 4130 (2003), doi:10.1063/1.1558205
9. M.A. Subramanian, N. Dong Li, Duan, B.A. Reisner, A.W. Sleight, *J. Solid State Chem.* **151**, 323 (2000) doi:10.1006/jssc.2000.8703
10. J. Liu, C.-G. Duan, W.-G. Yin, W.N. Mei, R.W. Smith, J.R. Hardy, *Phys. Rev. B* **70**, 144106 (2004), doi:10.1103/PhysRevB.70.144106
11. O. Bidault, M. Maglione, M. Actis, M. Kchikech, *Phys. Rev. B* **52**, 4191 (1995), doi:10.1103/PhysRevB.52.4191